Predictive Modelling of Glass Forming Ability in the Fe-Nb-B System Using the CALPHAD Approach

David D. E. Brennhaugen[a,*], Huahai Mao[b], Dmitri V. Louguine-Luzgin[c], Lars Arnberg[a] and Ragnhild E. Aune[a]

[a]*Department of Materials Science and Engineering, NTNU, Norwegian University of Science and Technology, 7491 Trondheim, Norway*
[b]*Department of Materials Science and Engineering, KTH Royal institute of Technology, 100 44 Stockholm, Sweden*
[c]*WPI Advanced Institute for Materials Research, Tohoku University, 2-1-1,Katahira, Sendai 980-8577, Japan*

Abstract

Accurate values needed for the most commonly used indicators of good Glass Forming Ability (GFA) in alloys, *i.e.* the liquidus (T_l), crystallization (T_x) and glass transition (T_g) temperatures, are only available after successful production of the metallic glass of interest. This has traditionally made discovery of new metallic glasses an expensive and tedious procedure, based on trial-and-error methodology.

The present study aims at testing the CALPHAD (Computer Coupling of Phase Diagrams and Thermochemistry) approach for predicting GFA in the Fe-Nb-B system by the use of the Thermo-Calc software and the thermodynamic database TCFE7. The melting temperatures and phase stabilities were calculated and combined with data for an atomic size mismatch factor, λ, in order to identify and map potential high-GFA regions. Selected compositions in the identified regions were later produced by suction casting and melt spinning, and the potential success verified using X-Ray Diffraction (XRD). Differential Scanning Calorimetry (DSC) was also used to compare thermodynamic calculations for the model predictions, and evaluate standard GFA indicators.

The model is found to fit well with literature data, as well as predict new bulk glassy compositions at and around $Fe_{70.5}Nb_7B_{22.5}$. These results show promise in further predictive use of the model.

Keywords: amorphous materials, metallic glasses, metals and alloys, rapid-solidification, GFA, computer simulations, CALPHAD

*Corresponding author: david.e.brennhaugen@ntnu.no

1 Introduction

Fe-based metallic glasses are of special interest due to their application as soft magnets in electronics.[1] Compared to standard electrical steel, which is commonly used for transformer cores, Fe-based metallic glasses show lower coercivity, higher permeability and resistivity, but somewhat lower saturation magnetization. Important factors hindering the widespread application of the amorphous alloys are, among others, their cost and the difficulty of designing or discovering new alloys.

Although several indicators of good Glass Forming Ability (GFA) are known, these often require after-the-fact analysis, still forcing the trial-and-error approach. The availability of a precise predictive modeling tool will therefore be very valuable in the further development of the field.

In the present study focus is on the Fe-Nb-B system, which was the first ternary Fe-based system in which a Bulk Metallic Glass (BMG), *i.e.* a fully amorphous rod with diameter of at least 1 mm, was sucessfully produced.[2][3] The availability of literature data on known compositions does therefore make the system a good candidate for testing a novel predictive modeling tool based on the CALPHAD (Computer Coupling of Phase Diagrams and Thermochemistry) approach.

The main aim of the present study has been to experimentally verify the viability of such a model, through the production of metallic glasses in both bulk and ribbon form. Thermal stability values obtained through DSC are used to evaluate the stability of the produced glasses in relation to the model.

2 Theory

The reduced glass transition temperature $T_{rg}=T_g/T_l$, where T_g and T_l are the glass transition temperature and the liquidus temperature respectively, is among the earliest proposed indicators of GFA.[4] Several similar indicators utilizing T_g, T_l, the solidification onset temperature (T_s) or crystallization temperature (T_x), *e.g.* $T_{rg}=T_g/T_s$, $\Delta T_x=T_x-T_g$, $\alpha=T_x/T_l$ *and* $\gamma=T_x/(T_g+T_l)$,[1] have later been proposed, suggesting that these values have at least some indicative power. While T_g remains relatively stable, T_l varies significantly with composition, and is therefore a powerful indicator during the design of new glassy alloys. Indeed most BMG are found at eutectic or near-eutectic compositions,[5] where T_l is depressed, making phase diagrams also an obvious tool during the alloy design phase.

The use of phase diagrams in the search for new metallic glasses is, however, limited to relatively simple systems, where an experimental mapping of temperatures and compositions exists. For more complex systems, which are generally required for good GFA, this approach is difficult. The CALPHAD methodology, which aims at developing models to represent thermodynamic properties for the various phases present in the system of interest, may therefore be used effectively to develop a satisfactory extrapolation of the relevant phase diagrams by mapping a limited number of experimental data points.

The Thermo-Calc software[6] is created using the CALPHAD methodology, and uses extensive thermodynamic databases of assessed systems to calculate the Gibbs free energies of all possible phases present in a system. Based on this, the stable phase at each composition and temperature may be predicted. The TCFE7 database, and other Thermo-Calc compatible thermodynamic descriptions available in literature,[7] contain the relevant thermodynamic information on the present Fe-Nb-B ternary system. A Liquidus projection of the Fe-rich corner of the Fe-Nb-B system, taken from Yoshitomi *et al.*[7] is shown in 1. However, as the TCFE7 database was developed mainly for applications in the steel-making industry, the system and its subsystems are not fulled assessed, *i.e.* some Nb-B binary and Fe-Nb-B ternary compounds are not included. Thus, the calculations performed in the present study using TCFE7 represent the metastable phase relations. The second set of calculations, based on an independently published thermodynamic description by Yoshitomi *et al.*[7] is therefore considered to be more reliable in this particular system, and are used to control the quality of the TCFE7 results.

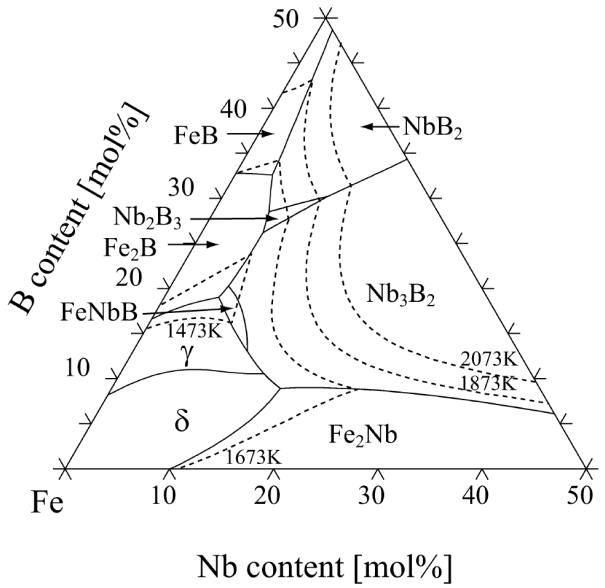

Figure 1: Liquidus projection of the Fe-rich corner in the Fe-Nb-B system, taken from Yoshitomi *et al.*[7]

In addition to thermodynamics, topological features may also be used effectively to predict glass formation. This effect has long been accounted for through the empirical requirement for constituent atoms with at least 12 % size difference.[8] A more continuous approach to the question of topology was introduced by Egami and Waseda in 1984[9] through the atomic mismatch factor, λ:

$$\lambda = c^B \left| \left(\frac{r_B}{r_A}\right)^3 - 1 \right| \qquad (1)$$

where c^B is the concentration of solute B in matrix A, and r^A and r^B the atomic radii of A and B respectively. By applying equation (1) they established that glass forming was possible at $\lambda \geq 0.1$ for the surveyed binary metallic glasses, and linked this to a critical lattice strain, caused by the volumetric mismatch of the species, required to suppress crystallization. The same concept was later extended to multi-component systems by Sá Lisboa *et al.*[10]

$$\lambda = \sum_{i=B}^{Z} c_i \left| \left(\frac{r_i}{r_A}\right)^3 - 1 \right| \qquad (2)$$

where i denotes the different solutes B through Z in matrix A.

Yan *et al.* [11] noted that optimal glass forming happens at $\lambda = 0.18$ for several investigated multi-component systems. When assuming that an amorphous material is made up of numerous clusters of icosahedra, the packing efficiency of these is shown to be at its peak at $\lambda = 0.18$.

Similarly, Miracle *et al*. [12] have used densely packed clusters of varying sizes with both substitutional and interstitial solutes to successfully predict glass forming compositions. This "efficiently packed clusters" model has gone far in pinpointing exact optimal locations for GFA based on topology alone.

While not taking the role of interstitial atoms into account, the λ-factors simplicity facilitates its combination with other indicative approaches. By combining information on the composition regions with

low liquidus temperatures, calculated by the Thermo-Calc software, with knowledge of the optimal λ-factor, a predictive model can be made which encompasses both topological and chemical effects.

3 Methodology

3.1 Model

In the present study Thermo-Calc version 2015a was used with the TCFE7 thermodynamic database, as well as the critically assessed data by Yoshitomi *et al.*[7], to model the ternary Fe-Nb-B phase diagram. An isothermal rendering at 1450 K of the area of interest, *i.e.* 10-30 at. % B, 0-10 at. % Nb, was used to locate the areas close to the peritectic line where liquid is still in equilibrium with one competing primary crystalline phase at low temperatures. Iso-λ lines from 0.10 to 0.20 were overlaid with the phase diagram to find the compositions with the highest topological susceptibility to glass forming. Two series of compositions were chosen along the two intersecting lines representing the lowest melting point and λ=0.18. The isothermal section of the Fe-Nb-B phase diagram at 1450 K, with overlaying iso-λ lines, can be seen in Figure 2. In the figure, the minimum solute content for expected successful production of amorphous compositions has also been identefied.

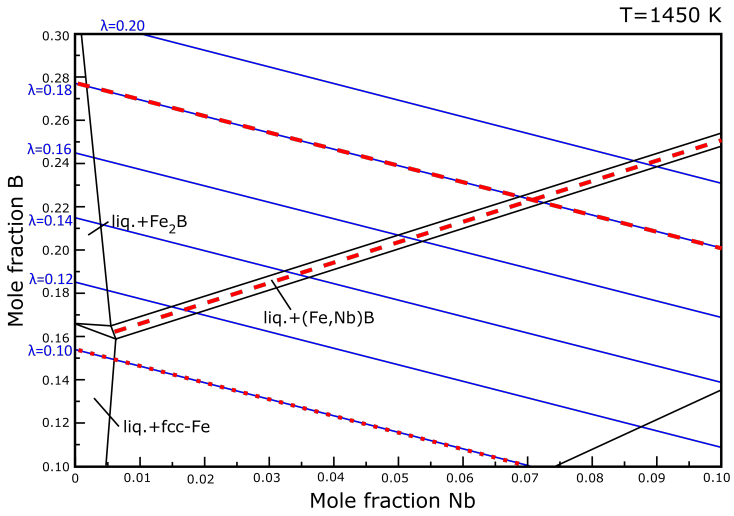

Figure 2: Isothermal section at 1450 K of the phase diagram Fe-Nb-B calculated by Thermo-Calc using TCFE7. Iso-λ lines are overlaid. Lines of expected maximal GFA are drawn in red dashes. Minimum λ value for successful amorhpous ribbons is marked with a red dotted line.

3.2 Sample production

High purity elements, Fe 99.99 mass % purity, Nb 99.9 mass % purity and B 99.5 mass % purity, were weighed with an error of maximum ± 0.2 %. Master alloy ingots of 5 g (10 g for melt spinner samples) were prepared by arc melting in Ar atmosphere (99.999 %) in an Edmund Bühler MAM-1 arc melter. Each ingot was turned and remelted five times to ensure compositional homogeneity.

Pieces of approximately 0.3 g each were used to cast 1 mm diameter rods in the suction caster module of the arc melter. Pieces of approximately 0.2 g were melt spun into 30 μm thick ribbons in Ar atmosphere (99.999 %) using a copper wheel with a surface velocity of 40 m/s.

3.3 Sample analysis

The structure of the produced materials was studied by X-Ray Diffraction (XRD) with Mo-Kα radiation (Bruker D8 Advance equipped with LynxEye detector) in Θ−2Θ mode.

Prior to analysis, the sample rods were polished lengthwise to a half-cylinder shape, and mounted in a capillary sample holder. By using a Soller slit, this method allows for selective analysis of various regions of the sample rod. The melt spun ribbons were cut into pieces and placed on a Si substrate sample holder. Both the wheel contact surface and the non-contact surface were analyzed to ensure full vitrification. Compositions which were established to be partially or fully crystalline were recast twice to ensure correct results.

Differential Scanning Calorimetry (DSC) was used to evaluate T_g, T_x, T_s and T_l values. Samples were measured for T_g and T_x during heating at 20 K/min, in the range of 303 to 1573 K, while T_s and T_l were found during cooling at the same rate in a NETZSCH STA449 Jupiter under Ar flow.

4 Results and Discussion

Based on the CAPHAD methodology high GFA is expected in low-T_l areas where the liquid extending from the Fe-B binany is in equilibrium with a stable Nb-B crystalline phase, while topology is proposed to be at its most beneficent along the 0.18 iso-λ line. It should therefore be expected to find the highest GFA values in the intersection of these two indicators. The locations of the samples produced in the present study are mapped out in the isothermal section of the generated Fe-Nb-B phase diagram, based on data from the TCFE7 database, presented in 3. As can be seen in the figure, a total of 14 compositions were cast into 1 mm rods, and four were produced as ribbons by melt spinning. Out of these, XRD confirmed seven rods with a completely amorphous cross section, and one amorphous ribbon. The XRD results for the fully amorphous bulk samples are shown in Figure 4**Error! Reference source not found.**.

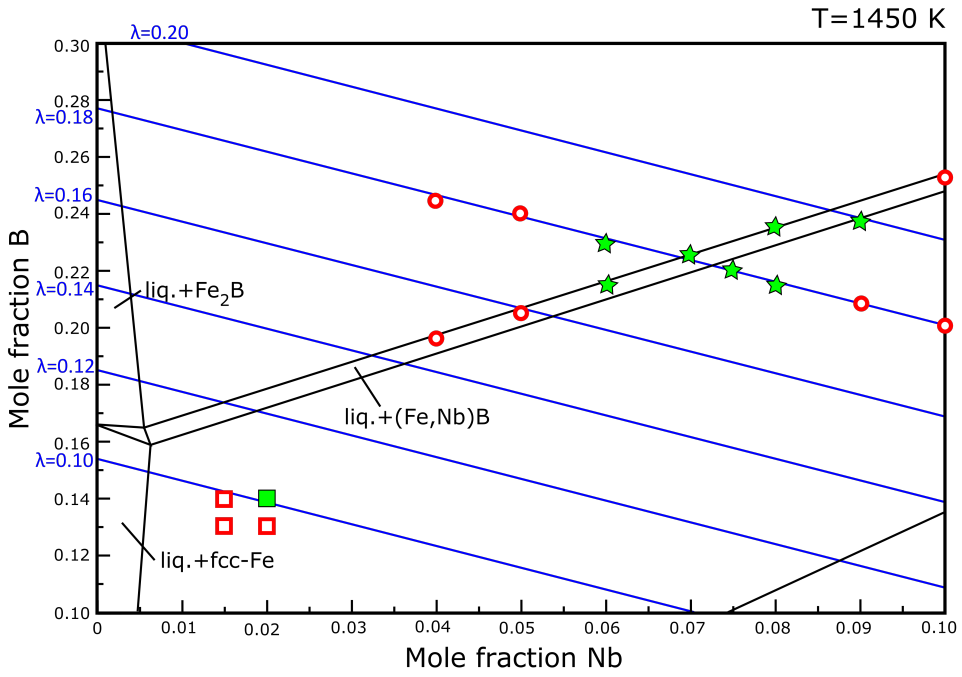

Figure 3: Isothermal section at 1450 K of the Fe-Nb-B phase diagram produced by Thermo-Calc using the TCFE7 database, overlaid with iso-λ lines and results from the present study. Fully amorphous rods and ribbons are marked as filled green stars and squares respectively. Partly or fully crystalline rods and ribbons are marked as open red circles and squares respectively.

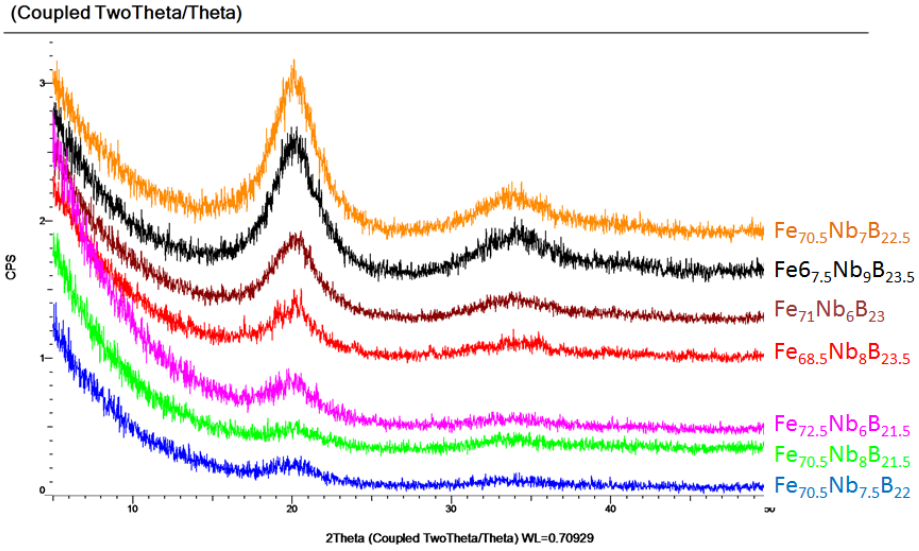

Figure 4: XRD plots of all successfully cast amorphous rods (all individually examined).

From 3 it can also be seen that the successfully produced glassy compositions are concentrated between λ=0.17 and λ=0.20, while at the same time being close to the peritectic line, in accordance with the assumptions of the model. The dividing line between amorphous and crystalline melt spun ribbons is at λ=0.10, as originally proposed by Egami and Waseda.[9]

The BMG compositions reported by Yao *et al.*[13] to exist in the in the Fe-Nb-B system coincide partly with those produced in the present study, as shown in Figure 5. The composition $Fe_{71}Nb_6B_{23}$ directly overlaps, while $Fe_{68.5}Nb_8B_{23.5}$, $Fe_{70.5}Nb_7B_{22.5}$ and $Fe_{72.5}Nb_6B_{21.5}$ are within 0.5 % B of previously reported glasses. The present authours failed to reproduce the amorphous $Fe_{71}Nb_5B_{24}$ alloy, but produced a fully amorphous $Fe_{70.5}Nb_8B_{21.5}$ alloy. The composition $Fe_{71}Nb_8B_{21}$ was, however, previously reported as crystalline. These discrepancies are believed to be attributable to differences in equipment, and individual variance in casting. The amorphous melt spun composition $Fe_{84}Nb_2B_{14}$ has previously been reported by Stoklosa *et al.*[14], together with $Fe_{87}Nb_2B_{11}$, which has a λ-value below 0.10 and was hence not expected to be amorphous. This suggests that the λ-factor used in the developed model does not signify an absolute limit.

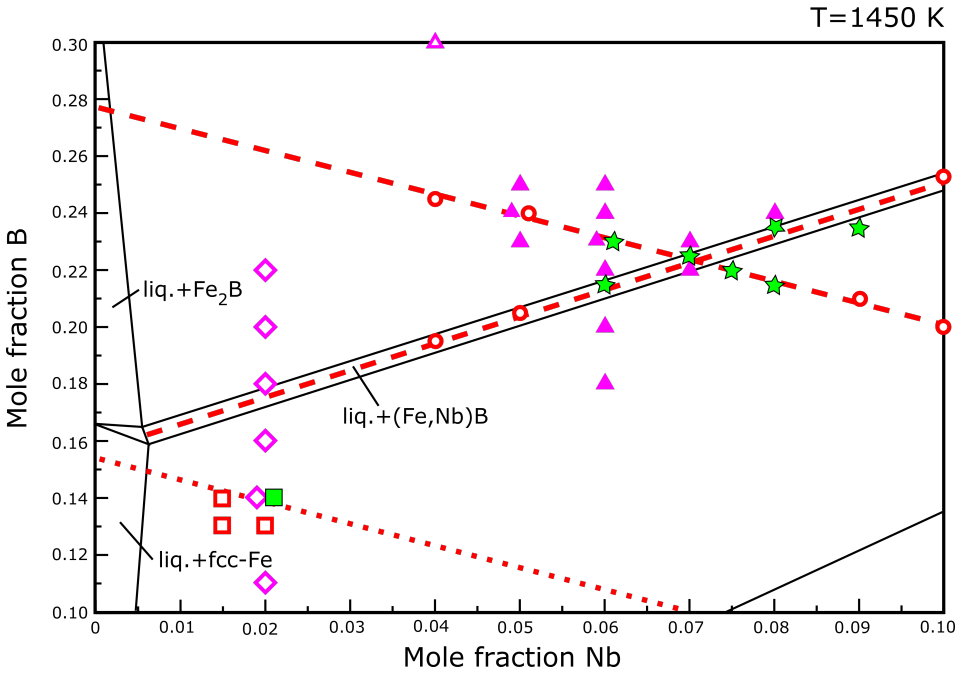

Figure 5: Isothermal section at 1450 K of the Fe-Nb-B phase diagram produced by Thermo-Calc using the TCFE7 database, overlaid with optimal(red dashes) and minimal(red dots) GFA lines. Results from the present work are compared to BMG and ribbons reported in literature. Fully amorphous rods and ribbons presently produced are marked as filled green stars and squares respectively. Crystalline rods and ribbons are marked as open red circles and squares respectively. The BMG compositions reported from literature are taken from Yao *et al.*[13] represented by purple filled triangles, and Stoica *et al.*[2] by purple open triangle. Melt spun ribbons,as reported by Stoklosa *et al.*[14] are marked as purple open diamonds.

In order to evaluate the trustworthiness of the TCFE7 database used in the present study, an additional phase diagram based on the specific critical assessment of the Fe-Nb-B system by Yoshitomi *et*

al.[7] was generated. An isothermal section at 1450 K of the assessed Fe-Nb-B phase diagram is presented in Figure 6, overlaid with the locations of samples produced in the present study. The desired multiphase region containing liquid can be seen to be wider than in the TCFE7 model at the same temperature, and its center is offset towards lower B content by about 3 at.%. The FeNbB phase present in the assessed phase diagram is not included in the TCFE7 database, which gives a metastable diagram with a solid solution of FeB and NbB, as well as an expected T_s value that is unrealistically high. The important aspect of the phase diagram is, however, the location of the peritectic line,which, with a 3 at.% offset, is still sufficient to identify potential high GFA in the present system.

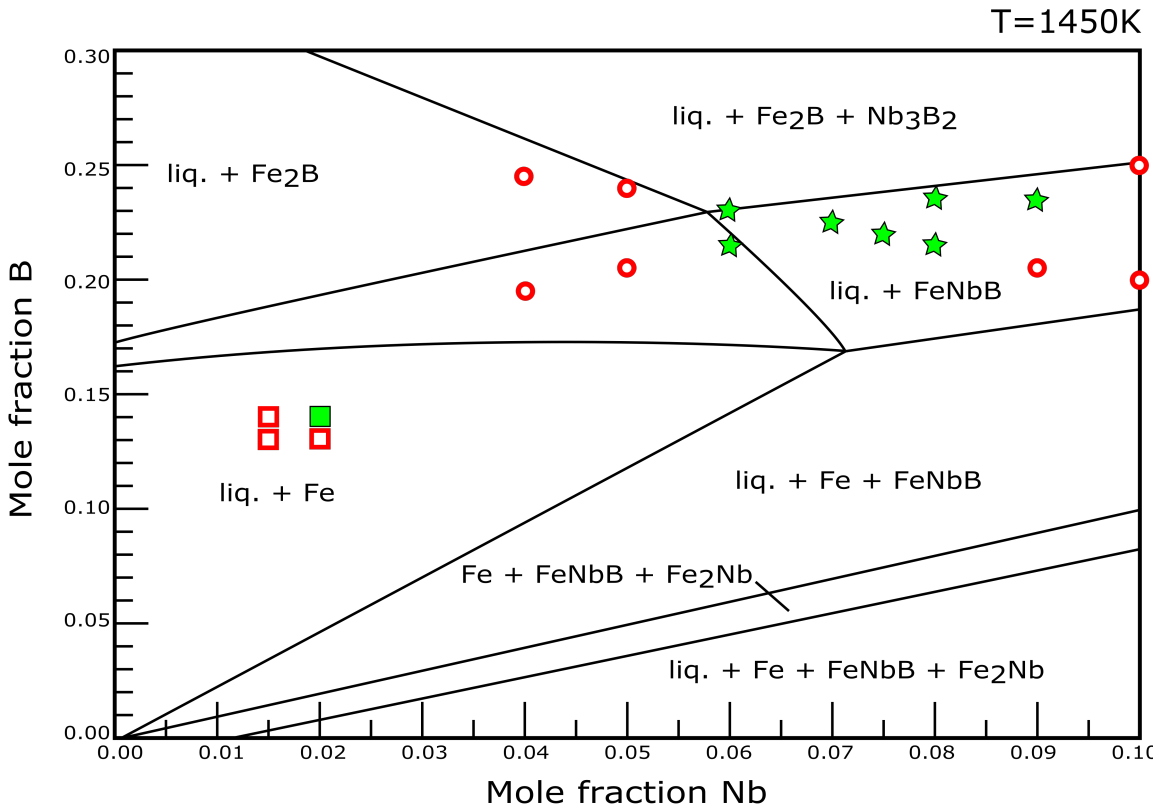

Figure 6: Isothermal section at 1450 K of the Fe-Nb-B phase diagram produced by Thermo-Calc using assessed data from Yoshitomi *et al.*[7] Results from the present study are marked (fully amorphous rods and ribbons as filled green stars and squares respectively, crystalline rods and ribbons as open red circles and squares respectively).

Thermodynamic stability parameters were evaluated by the use of DSC. A representative trace for the composition $Fe_{67.5}Nb_9B_{23.5}$, showing T_g, T_x, T_s and T_l can be seen in 7. The DSC results were used to calculate the GFA evaluation parameters T_{rg} and ΔT_g, see **Error! Reference source not found.**, as well as to compare actual values to those predicted by Thermo-Calc.

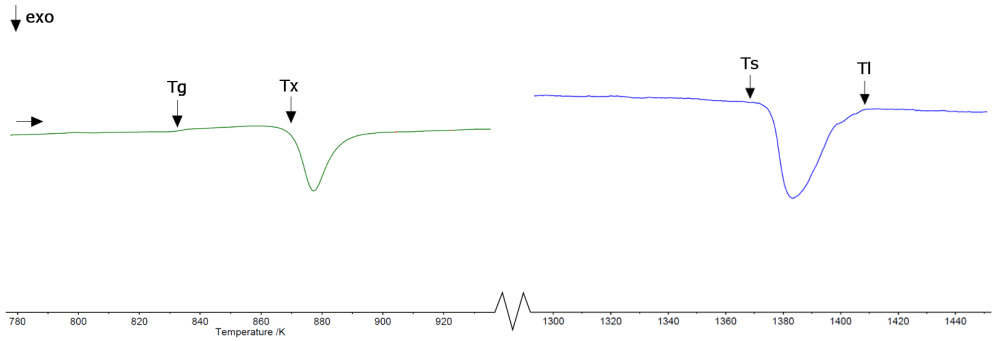

Figure 7: Representative DSC trace of $Fe_{67.5}Nb_9B_{23.5}$ with T_g, T_x, T_s and T_l values marked

As can be seen from Table 1, the DSC results indicate that T_g increases with an increase in the λ-factor, and highest values were found at the proposed optimum of λ=0.18. The DSC measured T_l values show a significant offset from the calculated equilibrium values, with deviations of up to 1173 K in the case of TCFE7 and 296 K for those based on Yoshitomi et al.[7]. Significantly, TCFE7 expects a drop in T_l from the BMG samples to the melt spun ribbon, while the assessed model correctly predicts an increase. Both models increase in accuracy towards the Fe corner of the phase diagram. Although the T_l temperatures are not quantitatively correctly predicted, the location of the peritectic line and the correllation with measured values is sufficient for use in the present model.

T_{rg} trends towards higher values with increasing λ, but with significant spread in values. Interestingly the lowest T_{rg} values are found in two λ=0.18 compositions, while higher T_{rg} is also found at similar compositions.

Table 1: Summary of thermodynamic values obtained through DSC and Thermo-Calc, as well as calculated GFA indicators T_{rg}, ΔT_x and λ

Composition	T_l	T_s	T_g	T_x	T_{rg}	ΔT_x	λ
$Fe_{67.5}Nb_9B_{23.5}$	1408	1369	832	870	0,59	38	0,198
$Fe_{68.5}Nb_8B_{23.5}$	1403	1342	835	888	0,60	53	0,193
$Fe_{70.5}Nb_8B_{21.5}$	1440	1341	838	857	0,58	19	0,180
$Fe_{70.5}Nb_{7.5}B_{22}$	1442	1330	831	866	0,58	35	0,181
$Fe_{70.5}Nb_7B_{22.5}$	1411	1355	829	861	0,59	32	0,181
$Fe_{71}Nb_6B_{23}$	1410	1357	838	859	0,59	21	0,180
$Fe_{72.5}Nb_6B_{21.5}$	1404	1355	821	846	0,58	25	0,170
$Fe_{84}Nb_2B_{14}$	1472	1345	651	672	0,44	21	0,101

The locations of the successfully produced amorphous alloys suggests that the indications from the model are of sufficient quality to be useful in searching for new BMG in the present system. The main

strength of the proposed predictive model derives from its ability to combine chemical factors, through the thermodynamic approach, with topology, from the λ-factor. The method itself is relatively simple to apply, as both the Thermo-Calc computations and the λ-calculations can be automated for a large number of systems, given access to the relevant databases. This could allow fast scanning of several complex systems for potential high-GFA compositions, guiding the experimental exploration. The potential for automatic scanning of alloy systems is also an important tool when working in systems with more than 3 components, which are not easily visualized for manual analysis. A sufficient database is still required to do precise models, which would be a limiting factor in what systems can be surveyed.

5 Conclusion

A predictive model for GFA in the Fe-Nb-B alloy system is proposed and tested. The CALPHAD methodology is used to locate areas of low T_l, and the data is combined with the atomic size mismatch factor λ, in order to identefy high-GFA areas. Based on the model, BMG of seven different compositions at and around $Fe_{70.5}Nb_7B_{22.5}$ were produced by suction casting, along with one glassy ribbon by melt spinning at $Fe_{84}Nb_2B_{14}$. The samples show good agreement with the predictions of the model, both in compositional location and in the thermodynamic stability evaluation. Six of the produced BMG compositions were previously unreported.

6 Acknowledgements

S. V. Ketov, V. Zadorozhnyy, K. Georgarakis and Z. Wang are acknowledged for assistance during the experimental work at WPI Advanced Institute for Materials Research, Tohoku University, Sendai, Japan. M. Stoika is acknowledged for valuable discussions. The research was funded by NTNU, Norwegian University of Science and Technology, Trondheim, Norway.

References

[1] C. Suryanarayana, A. Inoue, Iron-based bulk metallic glasses, Int. Mater. Rev. 58 (2013) 131–166.
[2] M. Stoica, K. Hajlaoui, A. LeMoulec, A.R. Yavari, New ternary Fe-based bulk metallic glass with high boron content, Philos. Mag. Lett. 86 (2006) 267–275.
[3] J.H. Yao, J.Q. Wang, Y. Li, Ductile Fe-Nb-B bulk metallic glass with ultrahigh strength, (2008).
[4] D. Turnbull, Under what conditions can a glass be formed?, Contemp. Phys. 10 (1969) 473–488. doi:10.1080/00107516908204405.
[5] H.S. Chen, Glassy metals, Reports Prog. Phys. 43 (1980) 353. http://iopscience.iop.org/0034-4885/43/4/001/pdf/0034-4885_43_4_001.pdf.
[6] J.-O. Andersson, T. Helander, L. Höglund, P. Shi, B. Sundman, Thermo-Calc & DICTRA, computational tools for materials science, Calphad. 26 (2002) 273–312.
[7] K. Yoshitomi, Y. Nakama, H. Ohtani, M. Hasebe, Thermodynamic analysis of the Fe-Nb-B ternary system, ISIJ Int. 48 (2008) 835–844.
[8] A. Inoue, Stabilization of metallic supercooled liquid and bulk amorphous alloys, Acta Mater. 48 (2000) 279–306.
[9] T. Egami, Y. Waseda, Atomic size effect on the formability of metallic glasses, J. Non. Cryst. Solids. 64 (1984) 113–134.
[10] R.D.S. Lisboa, C. Bolfarini, C.S. Kiminami, Topological instability as a criterion for design and selection of aluminum-based glass-former alloys, Appl. Phys. Lett. 86 (2005) 211904.
[11] Z.J. Yan, J.F. Li, S.R. He, Y.H. Zhou, Evaluation of the optimum solute concentration for good glass

forming ability in multicomponent metallic glasses, Mater. Res. Bull. 38 (2003) 681–689.
[12] D.B. Miracle, D. V Louzguine-Luzgin, L. V Louzguina-Luzgina, A. Inoue, An assessment of binary metallic glasses: Correlations between structure, glass forming ability and stability, Int. Mater. Rev. 55 (2010) 218–256.
[13] J.H. Yao, H. Yang, J. Zhang, J.Q. Wang, Y. Li, The influence of Nb and Zr on glass-formation ability in the ternary Fe–Nb–B and Fe–Zr–B and quaternary Fe–(Nb, Zr)–B alloy systems, J. Mater. Res. 23 (2008) 392–401.
[14] Z. Stokłosa, J. Rasek, P. Kwapuliński, G. Haneczok, A. Chrobak, J. Lelątko, L. Pająk, Influence of boron content on crystallization and magnetic properties of ternary FeNbB amorphous alloys, Phys. Status Solidi. 207 (2010) 452–456.

Captions

Figure 8: Liquidus projection of the Fe-rich corner in the Fe-Nb-B system, taken from Yoshitomi *et al.*[7]

Figure 9: Isothermal section at 1450 K of the phase diagram Fe-Nb-B calculated by Thermo-Calc using TCFE7. Iso-λ lines are overlaid. Lines of expected maximal GFA are drawn in red dashes. Minimum λ value for successful amorhpous ribbons is marked with a red dotted line.

Figure 10: Isothermal section at 1450 K of the Fe-Nb-B phase diagram produced by Thermo-Calc using the TCFE7 database, overlaid with iso-λ lines and results from the present study. Fully amorphous rods and ribbons are marked as filled green stars and squares respectively. Partly or fully crystalline rods and ribbons are marked as open red circles and squares respectively.

Figure 11: XRD plots of all successfully cast amorphous rods (all individually examined).

Figure 12: Isothermal section at 1450 K of the Fe-Nb-B phase diagram produced by Thermo-Calc using the TCFE7 database, overlaid with optimal(red dashes) and minimal(red dots) GFA lines. Results from the present work are compared to BMG and ribbons reported in literature. Fully amorphous rods and ribbons presently produced are marked as filled green stars and squares respectively. Crystalline rods and ribbons are marked as open red circles and squares respectively. The BMG compositions reported from literature are taken from Yao *et al.*[13] represented by purple filled triangles, and Stoica *et al.*[2] by purple open triangle. Melt spun ribbons,as reported by Stoklosa *et al.*[14] are marked as purple open diamonds.

Figure 13: Isothermal section at 1450 K of the Fe-Nb-B phase diagram produced by Thermo-Calc using assessed data from Yoshitomi *et al.*[7] Results from the present study are marked (fully amorphous rods and ribbons as filled green stars and squares respectively, crystalline rods and ribbons as open red circles and squares respectively).

Figure 14: Representative DSC trace of $Fe_{67.5}Nb_9B_{23.5}$ with T_g, T_x, T_s and T_l values marked

Table 2: Summary of thermodynamic values obtained through DSC and Thermo-Calc, as well as calculated GFA indicators T_{rg}, ΔT_x and λ